JOURNAL OF THERMOPHYSICS AND HEAT TRANSFER
Vol. 30, No. 1, January–March 2016

Polarization Dependence of the Reflectance and Transmittance of Anisotropic Metamaterials

Bo Zhao*
Georgia Institute of Technology, Atlanta, Georgia 30332-0405
Atsushi Sakurai†
Niigata University, Ikarashi, Niigata 950-2181, Japan
and
Zhuomin M. Zhang‡
Georgia Institute of Technology, Atlanta, Georgia 30332-0405

DOI: 10.2514/1.T4587

Due to the interference effect, the reflectance and transmittance of an arbitrary linearly polarized wave cannot be fully described by the reflectance and transmittance of transverse electric and transverse magnetic waves. In this work, the polarization dependence of reflectance and transmittance for anisotropic metamaterials is examined. The explicit mathematical relationship between the Fresnel coefficients and the reflectance (or transmittance) for a given polarization angle is derived. A method is presented that can be used to obtain the reflectance (or transmittance) for any polarization angle from three other polarizations. Several different anisotropic metamaterials are numerically investigated with the finite-difference time-domain technique to elucidate the polarization dependence of reflectance or transmittance. The reflectance and transmittance obtained from the three-polarization-angle method are in agreement with those from the rigorous numerical simulation.

Nomenclature

A, B, C	=	amplitude of the incident, reflected, or transmitted electric field, V/m
d	=	film thickness, m
$\boldsymbol{E}$	=	electric field, V/m
$\boldsymbol{H}$	=	magnetic field, A/m
h	=	height, m
i	=	$\sqrt{-1}$
$\boldsymbol{k}$	=	wave vector, m^{-1}
l	=	length, m
m	=	diffraction order in the x direction
n	=	diffraction order in the y direction
R	=	(directional-hemispherical) reflectance
$\boldsymbol{r}$	=	position vector, m
r	=	Fresnel's reflection coefficient
T	=	(directional-hemispherical) transmittance
t	=	Fresnel's transmission coefficient; time, s
w	=	width, m
ε	=	dielectric function
θ	=	polar angle, deg
Λ	=	grating period, m
λ	=	wavelength in vacuum, m
ϕ	=	azimuthal angle, deg
χ	=	phase angle, deg
ψ	=	polarization angle, deg
ω	=	angular frequency, rad/s

Subscripts

p	=	p polarization or transverse magnetic wave
s	=	s polarization or transverse electric wave

Superscripts

i	=	incidence
r	=	reflection
t	=	transmission

I. Introduction

PERIODIC nano/microstructures of various shapes have been used in metamaterial design [1–20] to manipulate light propagation. For metamaterial absorbers designed for energy-harvesting purposes, patterns with polarization-independent radiative properties may be preferred [1,6,13,21,22]. However, some shapes can induce a polarization-dependent response and can be used to design metamaterials with polarization control ability. These structures have recently attracted a lot of attention for their potential applications in plasmon-enhanced solar cells [11], nonlinear optics [23], holography [24], chemical sensing [25], one-way transmission [26,27], anomalous refraction [28], and Fano resonances [29]. Polarization-dependent emissivity can also be achieved using anisotropic metamaterials, since the emissivity is equal to the absorptivity following Kirchhoff's law [30]. Knowledge of thermal radiative properties is critical for applications such as material processing [31] and spacecraft thermal insulation [32,33]. Since the absorptivity can be obtained from the reflectance and transmittance by energy balance, the emissivity as a function of the polarization angle can be calculated once the polarization-dependent reflectance and transmittance are known. To determine the radiative properties of metamaterials with anisotropic shapes, it is important to understand the polarization-dependent reflectance and transmittance.

The reflectance and transmittance exhibit an extreme when eigenmodes are excited [34,35]; and for other polarizations, the reflectance and transmittance can be decomposed to that of the eigenmodes. Thus, it is critical to identify the eigenmodes associated with those shapes. To excite the eigenmodes, the incident wave should be at the eigenfrequency corresponding to the polarization status. For a metallic rod, the two eigenmodes can be excited at two eigenfrequencies when the electric field of the incident wave is along the long and short axes, respectively, and those two polarization states are the two eigenpolarizations. However, identifying the eigenpolarization can be very difficult when the shapes are asymmetrical.

Received 17 September 2014; revision received 27 January 2015; accepted for publication 31 January 2015; published online 26 March 2015.

*George W. Woodruff School of Mechanical Engineering.
†Department of Mechanical and Production Engineering.
‡George W. Woodruff School of Mechanical Engineering; zhuomin.zhang@me.gatech.edu (Corresponding Author).

Consider the film-coupled metamaterial structure shown in Fig. 1 under illumination of a linearly polarized plane wave. The unit cell is made of L-shape metal pattern of thickness h, separated from a metal ground plane by a dielectric film of thickness d. If the L shape is symmetric in the x and y directions (i.e., with respect to the diagonals), the reflectance of the transverse electric (TE) and transverse magnetic (TM) waves is equal for normal incidence. Here, the azimuthal angle ϕ for normal incidence is chosen to be 0 deg such that the $x-z$ plane defines the plane of incidence (POI). However, when the polarization angle ψ, which is the angle between the POI and the electric field of the incident wave, is rotated, the reflectance extrema appear at 45 and 135 deg [36], which are the eigenpolarizations of the symmetric structure. On the other hand, if the arms of the L shape are not equal ($l_x \neq l_y$), the dependence on polarization angle becomes more complicated and it becomes difficult to identify the eigenpolarizations. Though the matrix method for an anisotropic medium [37,38] may be applied for metamaterial analysis, obtaining the matrix can be difficult and it is more convenient if the reflectance and transmittance can be directly used to identify the eigenpolarizations. Thus, it is important to explore the relationship between the reflectance (transmittance) and the polarization angle for general anisotropic metamaterials.

For isotropic nonmagnetic materials, the reflectance of a linear polarized wave with a polarization angle ψ can be related to the reflectance of a transverse electric wave and a transverse magnetic wave by $R_\psi = R_{\mathrm{TE}} \sin^2\psi + R_{\mathrm{TM}} \cos^2\psi$; and the relation $R_{\mathrm{TM}} \leq R_\psi \leq R_{\mathrm{TE}}$ holds according to the Fresnel's coefficients [39]. However, these rules are not applicable for anisotropic metamaterials. The polarization-dependent reflectance or transmittance of anisotropic metamaterials has been observed by a number of researchers [2,8–11,18,34]. Chen et al. [8] investigated plasmonic switching and electromagnetically induced transparency with complex patterns. Cao et al. [9] studied the hybridized modes in a tri-rod nanostructure and polarization-dependent transmission. Husu et al. [34] discussed the eigenmodes in symmetric L-shape metamaterials based on the field distributions, but the way to identify the eigenmodes from reflectance (or transmittance) for asymmetric shapes was not addressed. Sung et al. [18] experimentally demonstrated polarization dependence and birefringence effects of a symmetric L-shape metamaterial. Nevertheless, the relationship between the reflectance (or transmittance) and the polarization angle for general anisotropic metamaterials is still unclear.

In the present work, analytical expression of the reflectance or transmittance of a linearly polarized incident plane wave is derived as a function of the polarization angle. The reflectance or transmittance extrema are presented. A three-polarization-angle method is proposed to obtain the reflectance or transmittance for any polarization angle using the reflectance or transmittance of TE, TM, and another polarization status. The results are compared with rigorous electromagnetic wave simulations using the finite difference time-domain (FDTD) method. Polarization-independent reflectance of metamaterials made of regular polygons is also demonstrated.

II. Reflection and Transmission

For reflection analysis, as shown in Fig. 1a, the direction of a linear polarized incidence is characterized by the incident wave vector $\boldsymbol{k}^i$ with polar angle θ and azimuthal angle ϕ, whereas the polarization angle $\psi(-\pi < \psi \leq \pi)$ describes the polarization status based on the angle between the POI and the electric field. Thus, TE and TM incident waves correspond to $\psi = 90$ and 0 deg, respectively. Due to the near-field coupling effect, the reflected wave generally has a different polarization status with the incident wave [40,41] and is generally elliptically polarized. Note that the focus of this study is on the reflection or transmission, and not the polarization status. For a plane wave with arbitrary polarization incident from a vacuum to a medium, the incident and reflected electric fields can be expressed as [37,42]

$$\boldsymbol{E}^i = (A_s\hat{\boldsymbol{s}}^i + A_p\hat{\boldsymbol{p}}^i)\exp(i\boldsymbol{k}^i \cdot \boldsymbol{r} - i\omega t) \tag{1}$$

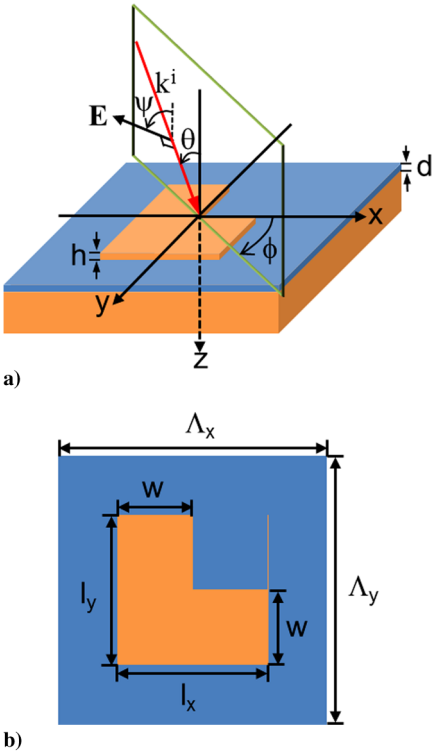

Fig. 1 The unit cell of the L-shape metal/dielectric/metal metamaterial: a) 3-D view b) top view.

$$\boldsymbol{E}^r = (B_s\hat{\boldsymbol{s}}^r + B_p\hat{\boldsymbol{p}}^r)\exp(i\boldsymbol{k}^r \cdot \boldsymbol{r} - i\omega t) \tag{2}$$

where superscripts i and r denote incidence and reflection, respectively; and $\hat{\boldsymbol{s}}$ and $\hat{\boldsymbol{p}}$ are the unit vectors in the electric field direction for TE (s-polarized) and TM (p-polarized) waves, respectively. It can be shown that

$$\hat{\boldsymbol{s}} = \frac{\boldsymbol{k}\times\hat{\boldsymbol{z}}}{|\boldsymbol{k}\times\hat{\boldsymbol{z}}|} \quad \text{and} \quad \hat{\boldsymbol{p}} = \frac{\hat{\boldsymbol{s}}\times\boldsymbol{k}}{|\hat{\boldsymbol{s}}\times\boldsymbol{k}|} \tag{3}$$

for either incident or reflected waves. Those two vectors can be used to describe the polarization status of incident and reflected waves, no matter whether they are linearly polarized or elliptically polarized. The general Fresnel's coefficients are defined by

$$r_{\alpha\beta} = B_\beta / A_\alpha \tag{4}$$

where $\alpha = s, p$ and $\beta = s, p$. The copolarized reflection coefficients are r_{ss} and r_{pp}, whereas the cross-polarized reflection coefficients are r_{sp} and r_{ps}. The first and second subscripts describe the polarization status of the reflected and incident waves, respectively. For an isotropic medium, no cross polarization can occur; thus, $r_{sp} = r_{ps} = 0$. Due to the anisotropy of the medium, in general, the reflected wave contains both s and p components, although the incident wave is either purely s or p polarized. Therefore, the reflectance consists of contributions from both TE and TM waves. For an incidence with polarization angle ψ and unit field amplitude, one obtains (by omitting the exponents)

$$\boldsymbol{E}^i_\psi = \sin\psi\hat{\boldsymbol{s}}^i + \cos\psi\hat{\boldsymbol{p}}^i \tag{5}$$

$$\boldsymbol{E}^r_\psi = (r_{ss}\sin\psi + r_{ps}\cos\psi)\hat{\boldsymbol{s}}^r + (r_{sp}\sin\psi + r_{pp}\cos\psi)\hat{\boldsymbol{p}}^r \tag{6}$$

Thus, the power reflectance is

$$R_\psi = |r_{ss}\sin\psi + r_{ps}\cos\psi|^2 + |r_{sp}\sin\psi + r_{pp}\cos\psi|^2$$
$$= R_{\mathrm{TE}}\sin^2\psi + R_{\mathrm{TM}}\cos^2\psi + R_C\sin(2\psi) \quad (7)$$

Here, $R_{\mathrm{TE}} = |r_{sp}|^2 + |r_{ss}|^2$ and $R_{\mathrm{TM}} = |r_{pp}|^2 + |r_{ps}|^2$ are the reflectance for the TE and TM waves, respectively; and $R_C = \mathrm{Re}(r_{ss}r_{ps}^*) + \mathrm{Re}(r_{pp}r_{sp}^*)$, which is generally nonzero but can be either positive or negative due to cross polarization. Note that the incidence medium discussed here is assumed lossless, and all the materials are nonmagnetic. Equation (7) can be recast as

$$R_\psi = A\sin(2\psi + \chi) + \bar{R} \quad (8)$$

where

$$A = \sqrt{(R_{\mathrm{TM}} - R_{\mathrm{TE}})^2/4 + R_C^2}$$

is the amplitude and $\bar{R} = (R_{\mathrm{TE}} + R_{\mathrm{TM}})/2$ is the average reflectance for TE and TM waves. The phase $\chi \in (-\pi, \pi]$ is determined by

$$\sin\chi = \frac{R_{\mathrm{TM}} - R_{\mathrm{TE}}}{2A} \quad \text{and} \quad \cos\chi = \frac{R_C}{A} \quad (9)$$

Thus, the reflectance is a periodic function of the polarization angle with a period of π. This is expected, since the response of the structure under an illumination polarized at $\psi + \pi$ can be obtained by that of ψ with a phase delay of π. Thus, the reflectance (or transmittance to be shown later) is the same. The reflectance averaged over all polarization angles is the same as the reflectance for an unpolarized (or randomly polarized) incident wave, viz.,

$$R_{\mathrm{unpolarized}} = \frac{1}{2\pi}\int_{-\pi}^{\pi} R_\psi\,\mathrm{d}\psi = \bar{R} \quad (10)$$

Thus, the reflectance of an unpolarized wave is equal to the average reflectance of TE and TM waves. In fact, for any two linearly polarized incident waves with orthogonal polarizations, their reflectance average is equal to the reflectance of an unpolarized wave.

Another interesting conclusion is that, due to the phase χ, the reflection extrema do not necessary occur at TE or TM polarization incidence. Based on Eq. (8), the reflection maximum and minimum actually occur at $\psi_1 = \pi/4 - \chi/2$ and $\psi_2 = \psi_1 + \pi/2$, respectively. After identifying the polarization status of the reflectance extrema, the reflectance for any polarizations can then be simply decomposed into the two reflection extrema as

$$R_\psi = R_{\max}\cos^2(\psi - \psi_1) + R_{\min}\sin^2(\psi - \psi_1) \quad (11)$$

where $R_{\max} = \bar{R} + A$ and $R_{\min} = \bar{R} - A$ are the reflection maximum and minimum, respectively. R_ψ follows an ellipse with a major axis of $2R_{\max}$ and a minor axis of $2R_{\min}$. Equation (11) is similar to decomposing the electromagnetic field, and thus offers a handy method for the calculation of the reflectance of an arbitrary polarization. Also, it can be seen that the difference of the polarization angles of the two reflection extrema is always 90 deg. If the reflectances of TE and TM waves are identical (i.e., $R_{\mathrm{TE}} = R_{\mathrm{TM}}$), then $\chi = 0$ or π, so that the two reflection extrema occur at $\psi = 45$ and 135 deg, respectively. However, it cannot be identified which one corresponds to the maxima because χ can be either 0 or π, depending on the sign of R_C. If R_C is positive, then $\chi = 0$ and the maxima occurs at $\psi_1 = 45$ deg; if R_C is negative, then $\chi = \pi$ and the maxima occurs at $\psi_1 = -45$ or 135 deg.

As an example, Fig. 2 plots the normal reflectance contours for the two structures as a function of the wavelength and polarization angle. The geometric structure is based on Fig. 1, and the parameters are as follows. Both of the metamaterial structures consist of a dielectric layer (Al_2O_3) of thickness $d = 140$ nm, sandwiched between an L-shape patterned 100-nm-thick gold layer and a gold ground plane that is opaque. The top metallic pattern repeats periodically in the x and y directions with the same period $\Lambda_x = \Lambda_y = 3.2$ μm. Also, the width is $w = 0.85$ μm and the y-direction length is $l_y = 1.7$ μm for both structures. The only difference between the two structures lies in the x-direction length: $l_x = 1.7$ μm (symmetric) for Fig. 2a; and $l_x = 1.275$ μm (asymmetric) for Fig. 2b. This difference results in a different polarization dependence between the two structures. The dielectric function of gold is obtained from [43], and the refractive index of Al_2O_3 is set to 1.6, which is a good approximation of sapphire in the spectral range of interest. For the normal incidence in the considered wavelength range, only zero-order diffraction (specular reflection) contributes to the reflectance, since all high-order terms are evanescent modes that are confined to the near-field regime of the subwavelength structure. A more general case will be discussed in Sec. III. The commercial Lumerical Solutions FDTD software was used to compute the reflectance of the metamaterial structures. Figure 2 shows the strong polarization dependence of the reflectance, especially at the wavelengths when the two resonances are excited. A detailed discussion of the magnetic polaritons that are responsible for the resonance absorption can be found in work by Sakurai et al. [36]. For Fig. 2a, the first and second resonances are at 5.7 and 8.1 μm, respectively, and they shift to 4.9 and 7.0 μm in Fig. 2b for the asymmetric L-shape structure due to the effect of a shorter arm length in the x direction. The polarization-dependent reflectance at the resonance wavelength is shown in the following as an illustration of the previous analysis and the three-polarization-angle method.

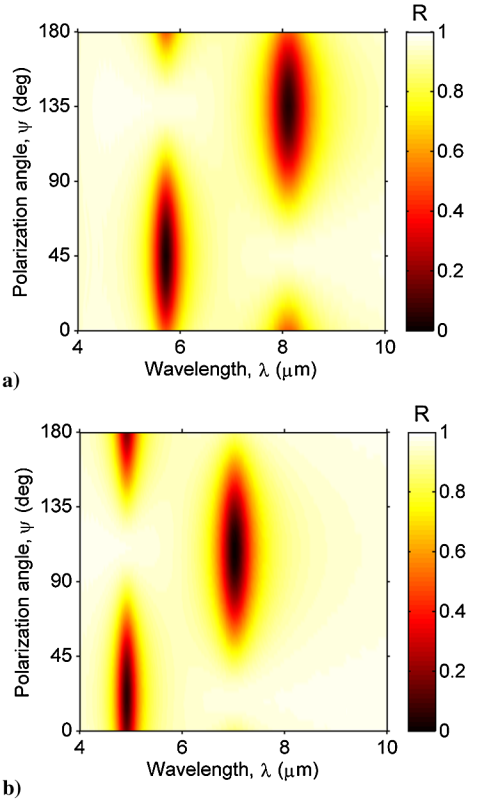

Fig. 2 Normal reflectance of two L-shape metamaterials: a) $l_x = l_y = 1.7$ μm; b) $l_x = 1.275$ μm; and $l_x = 1.7$ μm.

The structure with $l_x = l_y$ is symmetric along the diagonals; thus, the reflection extrema occur at $\psi = 45$ and 135 deg, as mentioned before. Furthermore, the reflectances of TE and TM waves are expected to be identical at normal incidence. This can be seen from Fig. 2a at $\psi = 0$ and 90 deg. For wavelengths of 5.7 and 8.1 μm, the values of R_{TE}, R_{TM}, and R_C can be obtained based on the reflection coefficients. For both wavelengths, R_{TE} is equal to R_{TM}; however, $R_C = -0.470$ for $\lambda = 5.7$ μm and $R_C = 0.457$ for $\lambda = 8.1$ μm. Thus, based on the previous discussion, the reflection maximum is at $\psi = 135$ deg for $\lambda = 5.7$ μm but 45 deg for $\lambda = 8.1$ μm. For the

second structure, since the symmetry is broken, the reflectances of TE and TM are not equal any more, as shown in Fig. 2b. Thus, the reflection extrema occur at polarization angles other than 45 or 135 deg. Using the Fresnel reflection coefficients from the simulation, one can calculate and show that the reflection maxima $R_{\max}$ occurs at 110 deg for $\lambda = 4.9$ μm and 18.6 deg for $\lambda = 7.0$ μm, as shown by the reflection contour in Fig. 2b.

Moreover, the polarization dependence of reflectance can be determined from the reflectance of three different polarization angles in the range $0 \le \psi < \pi$. For example, if R_{TE}, R_{TM}, and $R_{\psi'}$ are known, where ψ' is a polarization angle between 0 and 90 deg, the term R_C can be solved from Eq. (7). Furthermore, since the phase χ can also be determined, one can easily identify the polarization status of the reflectance extrema and then determine the eigenpolarizations. For instance, the reflectance for the second structure at $\lambda = 7.0$ μm and $\psi = 45$ deg is 0.774. Using this value together with R_{TE} and R_{TM}, one can obtain $R_C = 0.289$, which is the same as obtained from Fresnel's reflection coefficients. Furthermore, $R_{\max} = 0.964$, $R_{\min} = 0.006$, and $\psi_1 = 18.6$ deg can also be determined. Then, the reflectance as a function of the polarization angle can be accurately obtained using either Eqs. (7), (8), or (11), as shown in Fig. 3 with markers, along with the results for $\lambda = 4.9$ μm using the same procedure. If the reflection spectra for TE, TM, and another polarization can be obtained from simulations or experiments, then the same calculation can be repeated for each wavelength; thus, the reflection contours shown in Figs. 2a and 2b can be reproduced based on the three-polarization-angle method.

For a semitransparent subwavelength periodic structure, under the same incident wave as described by Eq. (1) and illustrated in Fig. 1a, the transmitted electric field can be expressed as

$$\boldsymbol{E}^t = (C_s\hat{\boldsymbol{s}}^t + C_p\hat{\boldsymbol{p}}^t)\exp(i\boldsymbol{k}^t\cdot\boldsymbol{r} - i\omega t) \tag{12}$$

where the superscript t denotes transmission, and $\hat{\boldsymbol{s}}$ and $\hat{\boldsymbol{p}}$ are defined in terms of the wave vector of the transmitted wave similar to the reflected wave. The general Fresnel transmission coefficients are defined by $t_{\alpha\beta} = C_\beta/A_\alpha$, where $\alpha = s, p$ and $\beta = s, p$. For an incidence with polarization angle ψ and unit field amplitude as expressed in Eq. (5), one obtains

$$\boldsymbol{E}^t_\psi = (t_{ss}\sin\psi + t_{ps}\cos\psi)\hat{\boldsymbol{s}}^t + (t_{sp}\sin\psi + t_{pp}\cos\psi)\hat{\boldsymbol{p}}^t \tag{13}$$

Thus, the power transmittance is [39,40]

$$T_\psi = |t_{ss}\sin\psi + t_{ps}\cos\psi|^2\mathrm{Re}\left(\frac{k^t_z}{k^i_z}\right) + |t_{sp}\sin\psi + t_{pp}\cos\psi|^2\mathrm{Re}\left(\frac{\varepsilon^i k^t_z}{\varepsilon^t k^i_z}\right) \tag{14}$$

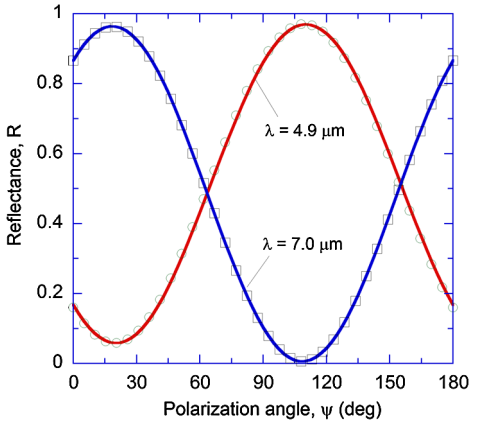

Fig. 3 Comparison of the normal reflectance calculated from FDTD (curves) and the three-polarization-angle method (markers).

where ε is the dielectric function, and k_z is the z component of the wave vector. By defining

$$T_{\mathrm{TE}} = \mathrm{Re}\left(\frac{\varepsilon^i k^t_z}{\varepsilon^t k^i_z}\right)|t_{sp}|^2 + \mathrm{Re}\left(\frac{k^t_z}{k^i_z}\right)|t_{ss}|^2 \tag{15}$$

$$T_{\mathrm{TM}} = \mathrm{Re}\left(\frac{\varepsilon^i k^t_z}{\varepsilon^t k^i_z}\right)|t_{pp}|^2 + \mathrm{Re}\left(\frac{k^t_z}{k^i_z}\right)|t_{ps}|^2 \tag{16}$$

and

$$T_C = \mathrm{Re}\left(\frac{\varepsilon^i k^t_z}{\varepsilon^t k^i_z}\right)\mathrm{Re}(t_{pp}t^*_{sp}) + \mathrm{Re}\left(\frac{k^t_z}{k^i_z}\right)\mathrm{Re}(t_{ss}t^*_{ps}) \tag{17}$$

Eq. (14) can be written as

$$T_\psi = T_{\mathrm{TE}}\sin^2\psi + T_{\mathrm{TM}}\cos^2\psi + T_C\sin(2\psi) \tag{18}$$

Here, T_{TE} and T_{TM} are the transmittance for TE and TM waves, respectively. Since Eq. (18) has the same form as Eq. (7), all the previous discussions for reflection can be repeated for the transmittance. Hence, the transmittance is also a sinusoidal function of the polarization angle. Here, two metamaterial surfaces in a vacuum environment made of L shapes are used to demonstrate the transmittance as a function of the polarization angle in the same coordinate as with the reflectance analysis. Those metamaterial surfaces are made of the same L-shape gold patterns as shown in Fig. 1, without the dielectric layer and the ground plane. The normal transmittance contours are shown in Figs. 4a and 4b for $l_x = 1.7$ and 1.275 μm, respectively, keeping the period, thickness, and y-directional length the same as for Fig. 2. The resonance at $\lambda = 3.2$ μm is due to surface plasmon polaritons [3], and the other two resonances can be attributed to the localized plasmonic resonances associated with the L shape [34]. Due to the relatively short arm in the x direction, the two localized resonances shift toward shorter wavelengths in Fig. 4b compared with Fig. 4a. Due to symmetry, the transmittance extrema in Fig. 4a occur at $\psi = 45$ and 135 deg, but they are at about $\psi = 110$ and 20 deg for Fig. 4b at $\lambda = 3.2$ μm. These results can also be obtained with the three-polarization-angle method from the transmittance of TE, TM, and another polarization. The contour plots can thus be reproduced if the transmittance at three different polarization angles is known at each wavelength. The procedure is similar to that for the reflectance and will not be repeated here. Note that the preceding analysis is valid for all incident directions and not just the normal direction, even though the reflectance and transmittance contours shown here are for normal incidence.

III. Diffraction with Multiple Propagating Orders

The preceding discussion assumes that only the zero-order (specular) diffracted wave is a propagating wave, whereas all high orders are evanescent waves that do not carry energy in the far field. As discussed next, this assumption is not necessary and the diffraction efficiency for each order as well as the directional-hemispherical reflectance for diffracted waves follow a similar trend. This still holds for practical fabricated structures as long as scattering due to surface roughness, inhomogeneity, and other irregularities is negligibly small [44].

At large incident angles, the two-dimensional periodic metamaterial structure, shown in Fig. 1, can reflect multiple propagating waves that are not necessarily in the POI but in the planes of diffraction [3,40]. These diffraction orders may be denoted as m and n in the x and y directions, respectively. If the incident wave is described by Eq. (5), then the electric field of the mn-th reflected order can be expressed as

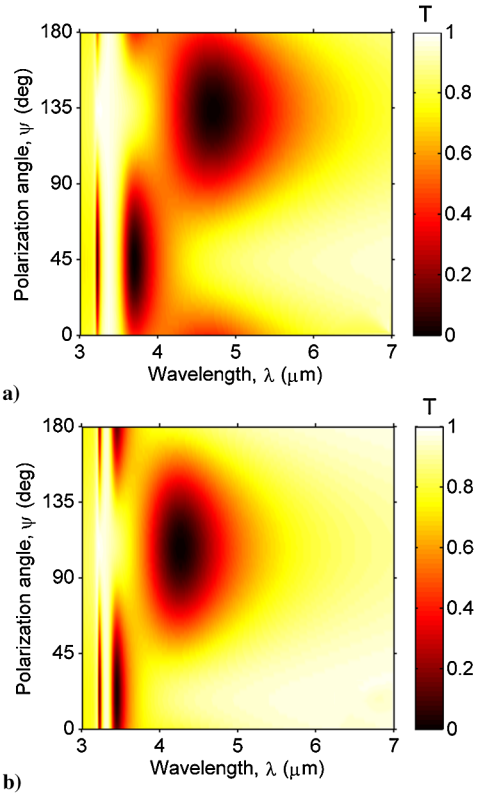

Fig. 4 Normal transmission for two *L*-shape metamaterial surfaces: a) $l_x = 1.7\ \mu$m; b) $l_x = 1.275\ \mu$m.

$$\boldsymbol{E}^r_{\psi,mn} = (r_{ss,mn}\sin\psi + r_{ps,mn}\cos\psi)\hat{\boldsymbol{s}}^r_{mn} + (r_{sp,mn}\sin\psi + r_{pp,mn}\cos\psi)\hat{\boldsymbol{p}}^r_{mn} \tag{19}$$

where $\hat{\boldsymbol{s}}_{mn}$ and $\hat{\boldsymbol{p}}_{mn}$ are defined similar to $\hat{\boldsymbol{s}}$ and $\hat{\boldsymbol{p}}$ but are in terms of the wave vector of the mn-th reflected order. Thus, the diffraction efficiency (DE) can be obtained as [40]

$$DE^r_{\psi,mn} = R_{\mathrm{TE},mn}\sin^2\psi + R_{\mathrm{TM},mn}\cos^2\psi + R_{C,mn}\sin(2\psi) \tag{20}$$

where

$$R_{\mathrm{TE},mn} = \mathrm{Re}\left(\frac{k^r_{z,mn}}{k^i_z}\right)(|r_{sp,mn}|^2 + |r_{ss,mn}|^2)$$

$$R_{\mathrm{TM},mn} = \mathrm{Re}\left(\frac{k^r_{z,mn}}{k^i_z}\right)(|r_{pp,mn}|^2 + |r_{ps,mn}|^2)$$

and

$$R_{C,mn} = \mathrm{Re}\left(\frac{k^r_{z,mn}}{k^i_z}\right)[\mathrm{Re}(r_{ss,mn}r^*_{ps,mn}) + \mathrm{Re}(r_{pp,mn}r^*_{sp,mn})]$$

Equation (20) has the same form as Eq. (7); therefore, the DE for each order is a sinusoidal function of the polarization angle with a period of π. However, the phase and diffraction efficiency extrema would, in general, be different for different orders, though the diffraction efficiency extrema still occur at a pair of orthogonal polarization states for different orders. For example, Fig. 5 illustrates the DE as a function of the polarization angle for the second structure with $\phi = 0$ and $\theta = 45$ deg. In this direction, the (0, 0) and $(-1, 0)$ orders of the reflected wave are propagating and they have different phases, as the figure shows. The directional-hemispherical reflectance (DHR) (or, simply, reflectance) can be obtained by adding the DE of each order:

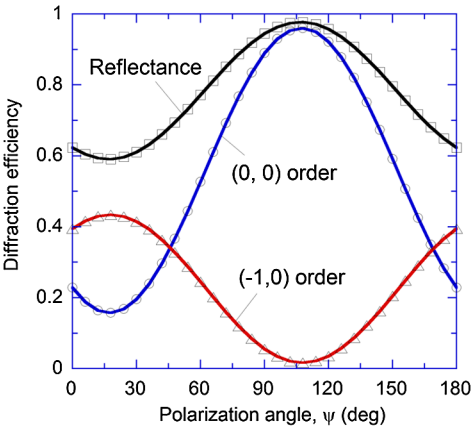

Fig. 5 Reflectance and DEs at $\lambda = 4.9\ \mu$m predicted from FDTD and reproduced from the three-polarization-angle method (markers).

$$R_\psi = \sum_{m,n} \mathrm{DE}^r_{\psi,mn} = R_{\mathrm{TE}}\sin^2\psi + R_{\mathrm{TM}}\cos^2\psi + R_C\sin(2\psi) \tag{21}$$

where R_{TE}, R_{TM}, and R_C are the summation of $R_{\mathrm{TE},mn}$, $R_{\mathrm{TM},mn}$, and $R_{C,mn}$ of all orders. Therefore, R_{TE} and R_{TM} are the reflectances of TE and TM waves, respectively. Equation (21) is similar to Eq. (7), where only one order is propagating; thus, the DHR is always a sinusoidal function. Similarly, the DHR and DE can be reproduced by using the three-polarization-angle method from the DHR and DEs of three different polarizations. For instance, the markers in Fig. 5 show the reproduced results by using the reflectance and DEs for TE, TM, and $\psi = 45$ deg. The results obtained from the three-polarization-angle method match the results of the direct simulations exactly.

For semitransparent metamaterials that have multiple transmission orders, if the incident wave is expressed as in Eq. (5), the transmitted electric field for the mn-th order can be obtained by

$$\boldsymbol{E}^t_{\psi,mn} = (t_{ss,mn}\sin\psi + t_{ps,mn}\cos\psi)\hat{\boldsymbol{s}}^t_{mn} + (t_{sp,mn}\sin\psi + t_{pp,mn}\cos\psi)\hat{\boldsymbol{p}}^t_{mn} \tag{22}$$

where $\hat{\boldsymbol{s}}_{mn}$ and $\hat{\boldsymbol{p}}_{mn}$ are defined similar to $\hat{\boldsymbol{s}}$ and $\hat{\boldsymbol{p}}$ but are in terms of the wave vector of the mn-th transmission order. Thus, the DE for transmitted waves is [40]

$$\mathrm{DE}^t_{\psi,mn} = T_{\mathrm{TE},mn}\sin^2\psi + T_{\mathrm{TM},mn}\cos^2\psi + T_{C,mn}\sin(2\psi) \tag{23}$$

where

$$T_{\mathrm{TE},mn} = \mathrm{Re}\left(\frac{\varepsilon^i k^t_{z,mn}}{\varepsilon^t k^i_z}\right)|t_{sp,mn}|^2 + \mathrm{Re}\left(\frac{k^t_{z,mn}}{k^i_z}\right)|t_{ss,mn}|^2,$$

$$T_{\mathrm{TM},mn} = \mathrm{Re}\left(\frac{\varepsilon^i k^t_{z,mn}}{\varepsilon^t k^i_z}\right)|t_{pp,mn}|^2 + \mathrm{Re}\left(\frac{k^t_{z,mn}}{k^i_z}\right)|t_{ps,mn}|^2$$

and

$$T_{C,mn} = \mathrm{Re}\left(\frac{\varepsilon^i k^t_{z,mn}}{\varepsilon^t k^i_z}\right)\mathrm{Re}(t_{pp,mn}t^*_{sp,mn}) + \mathrm{Re}\left(\frac{k^t_{z,mn}}{k^i_z}\right)\mathrm{Re}(t_{ss,mn}t^*_{ps,mn})$$

Equation (23) has the same form as Eq. (20); thus, the conclusions for reflection DEs also hold for transmission DEs.

Furthermore, since the reflectance is a sinusoidal function of the polarization angle, if three different polarization angles that have the same reflectance can be found in the range $0 \le \psi < \pi$, then $R_{\mathrm{TE}} = R_{\mathrm{TM}}$ and $R_C = 0$. Thus, the reflectance becomes independent of polarization angle. For instance, the *L*-shape pattern in Fig. 1 is

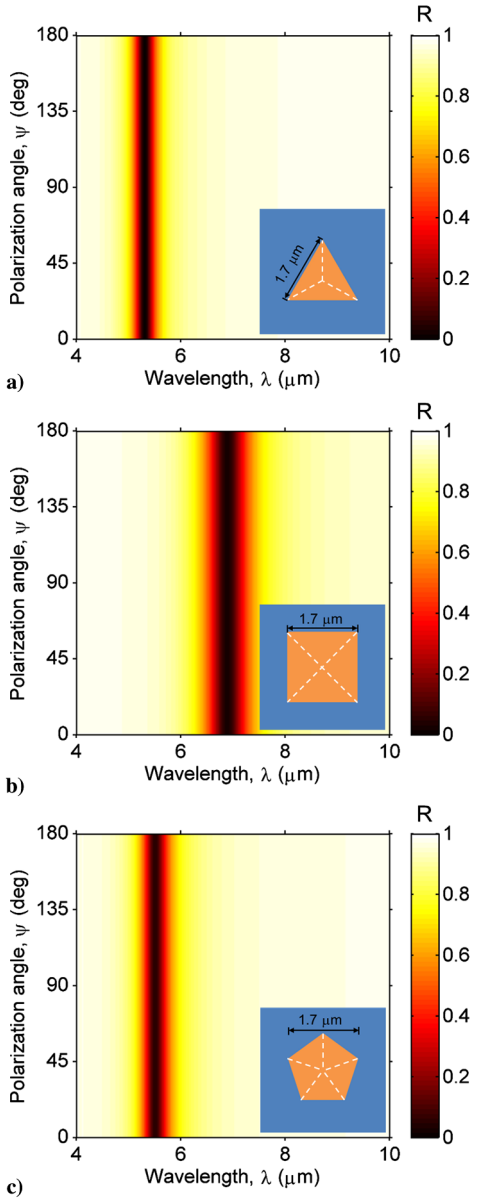

Fig. 6 Normal reflectance for structures with different patterns: a) equilateral triangles; b) squares; and c) regular pentagons.

replaced by regular polygon patterns, as shown in the insets of Fig. 6a to 6c, where an equilateral triangle, a square, and a regular pentagon pattern are used, respectively. Due to the symmetry, the reflectance at normal incidence is expected to be equal when the electric field of the incident wave is along the directions of 45 and 135 deg. A third polarization angle (e.g., 90 deg) can be used to check the polarization dependence. As it turned out, the normal reflectance is polarization independent; this is also confirmed by the contour plots shown in Fig. 6, obtained from the FDTD simulations. Other symmetrically patterned structures like crosses [12] and fishnets [21] also exhibit polarization independence. Similar rules also hold for semitransparent anisotropic metamaterials for which the transmission is of interest.

IV. Conclusions

The reflectance and transmittance of a linear polarized wave are shown to be sinusoidal functions of the polarization angle. The two reflectance (or transmittance) extrema occur at a pair of orthogonal polarization states called eigenpolarizations. Furthermore, for an arbitrary polarization status, the reflectance and transmittance, as well as the diffraction efficiency of each diffracted order, can be determined using the three-polarization-angle method. This work helps the understanding of the polarization dependence of reflectance or transmittance of anisotropic nanostructures and facilitates the investigation of the eigenresonances in metamaterial structures and their potential applications for polarization control.

Acknowledgments

This work was primarily supported by the National Science Foundation (CBET-1235975). Z. M. Zhang was also supported by the U.S. Department of Energy, Office of Science, Basic Energy Sciences (DE-FG02-06ER46343).

References

[1] Grant, J., Ma, Y., Saha, S., Khalid, A., and Cumming, D. R. S., "Polarization Insensitive, Broadband Terahertz Metamaterial Absorber," *Optics Letters*, Vol. 36, No. 17, 2011, pp. 3476–3478. doi:10.1364/OL.36.003476

[2] Canfield, B. K., Kujala, S., Jefimovs, K., Vallius, T., Turunen, J., and Kauranen, M., "Polarization Effects in the Linear and Nonlinear Optical Responses of Gold Nanoparticle Arrays," *Journal of Optics A: Pure and Applied Optics*, Vol. 7, No. 2, 2005, Paper S110. doi:10.1088/1464-4258/7/2/015

[3] Zhao, B., Wang, L. P., Shuai, Y., and Zhang, Z. M., "Thermophotovoltaic Emitters Based on a Two-Dimensional Grating/Thin-Film Nanostructure," *International Journal of Heat and Mass Transfer*, Vol. 67, Dec. 2013, pp. 637–645. doi:10.1016/j.ijheatmasstransfer.2013.08.047

[4] Sakurai, A., Zhao, B., and Zhang, Z. M., "Resonant Frequency and Bandwidth of Metamaterial Emitters and Absorbers Predicted by an RLC Circuit Model," *Journal of Quantitative Spectroscopy and Radiative Transfer*, Vol. 149, Dec. 2014, pp. 33–40. doi:10.1016/j.jqsrt.2014.07.024

[5] Tok, R. U., Ow-Yang, C., and Şendur, K., "Unidirectional Broadband Radiation of Honeycomb Plasmonic Antenna Array with Broken Symmetry," *Optics Express*, Vol. 19, No. 23, 2011, pp. 22,731–22,742. doi:10.1364/OE.19.022731

[6] Wang, H., and Wang, L. P., "Perfect Selective Metamaterial Solar Absorbers," *Optics Express*, Vol. 21, No. S6, 2013, pp. A1078–A1093. doi:10.1364/OE.21.0A1078

[7] Bossard, J. A., and Werner, D. H., "Metamaterials with Angle Selective Emissivity in the Near-Infrared," *Optics Express*, Vol. 21, No. 5, 2013, pp. 5215–5225. doi:10.1364/OE.21.005215

[8] Chen, J. X., Wang, P., Chen, C., Lu, Y., Ming, H., and Zhan, Q., "Plasmonic EIT-Like Switching in Bright-Dark-Bright Plasmon Resonators," *Optics Express*, Vol. 19, No. 7, 2011, pp. 5970–5978. doi:10.1364/OE.19.005970

[9] Cao, J. X., Liu, H., Li, T., Wang, S. M., Li, T. Q., Zhu, S. N., and Zhang, X., "Steering Polarization of Infrared Light Through Hybridization Effect in a Tri-Rod Structure," *Journal of the Optical Society of America B*, Vol. 26, No. 12, 2009, pp. B96–B101. doi:10.1364/JOSAB.26.000B96

[10] Cao, J. X., Liu, H., Li, T., Wang, S. M., Dong, Z. G., and Zhu, S. N., "High Sensing Properties of Magnetic Plasmon Resonance in the Double-Rod and Tri-Rod Structures," *Applied Physics Letters*, Vol. 97, No. 7, 2010, Paper 071905. doi:10.1063/1.3481359

[11] Tok, R. U., and Şendur, K., "Absorption Efficiency Enhancement in Inorganic and Organic Thin Film Solar Cells via Plasmonic Honeycomb Nanoantenna Arrays," *Optics Letters*, Vol. 38, No. 16, 2013, pp. 3119–3122. doi:10.1364/OL.38.003119

[12] Liu, X., Starr, T., Starr, A. F., and Padilla, W. J., "Infrared Spatial and Frequency Selective Metamaterial with Near-Unity Absorbance," *Physical Review Letters*, Vol. 104, No. 20, 2010, Paper 207403. doi:10.1103/PhysRevLett.104.207403

[13] Hao, J., Wang, J., Liu, X., Padilla, W. J., Zhou, L., and Qiu, M., "High Performance Optical Absorber Based on a Plasmonic Metamaterial," *Applied Physics Letters*, Vol. 96, No. 25, 2010, Paper 251104. doi:10.1063/1.3442904

[14] Zhang, B., Zhao, Y., Hao, Q., Kiraly, B., Khoo, I.-C., Chen, S., and Huang, T. J., "Polarization-Independent Dual-Band Infrared Perfect Absorber Based on a Metal-Dielectric-Metal Elliptical Nanodisk Array," *Optics Express*, Vol. 19, No. 16, 2011, pp. 15,221–15,228. doi:10.1364/OE.19.015221

[15] Chen, K., Adato, R., and Altug, H., "Dual-Band Perfect Absorber for Multispectral Plasmon-Enhanced Infrared Spectroscopy," *ACS Nano*,

Vol. 6, No. 9, 2012, pp. 7998–8006.
doi:10.1021/nn3026468
[16] Liu, N., Liu, H., Zhu, S., and Giessen, H., "Stereometamaterials," *Nature Photonics*, Vol. 3, No. 3, 2009, pp. 157–162.
doi:10.1038/nphoton.2009.4
[17] Qiu, J., Hsu, P.-F., and Liu, L. H., "Infrared Radiative Properties of Two-Dimensional Square Optical Black Holes with Materials of Insulators and Semiconductors," *Journal of Quantitative Spectroscopy and Radiative Transfer*, Vol. 132, Jan. 2014, pp. 99–108.
doi:10.1016/j.jqsrt.2013.01.028
[18] Sung, J., Sukharev, M., Hicks, E. M., Van Duyne, R. P., Seideman, T., and Spears, K. G., "Nanoparticle Spectroscopy: Birefringence in Two-Dimensional Arrays of L-Shaped Silver Nanoparticles," *Journal of Physical Chemistry C*, Vol. 112, No. 9, 2008, pp. 3252–3260.
doi:10.1021/jp077389y
[19] Chen, J. X., and Hu, J., "Strong Coupling between Localized and Propagating Surface Plasmon Modes in a Noncentrosymmetric Metallic Photonic Slab," *Journal of the Optical Society of America B*, Vol. 31, No. 7, 2014, pp. 1600–1606.
doi:10.1364/JOSAB.31.001600
[20] Yu, N., Genevet, P., Aieta, F., Kats, M. A., Blanchard, R., Aoust, G., Tetienne, J.-P., Gaburro, Z., and Capasso, F., "Flat Optics: Controlling Wavefronts with Optical Antenna Metasurfaces," *IEEE Journal of Selected Topics in Quantum Electronics*, Vol. 19, No. 3, 2013, Paper 4700423.
doi:10.1109/JSTQE.2013.2241399
[21] Aydin, K., Ferry, V. E., Briggs, R. M., and Atwater, H. A., "Broadband Polarization-Independent Resonant Light Absorption Using Ultrathin Plasmonic Super Absorbers," *Nature Communications*, Vol. 2, Nov. 2011, Article No 517.
doi:10.1038/ncomms1528
[22] Nguyen-Huu, N., Chen, Y.-B., and Lo, Y.-L., "Development of a Polarization-Insensitive Thermophotovoltaic Emitter with a Binary Grating," *Optics Express*, Vol. 20, No. 6, 2012, pp. 5882–5890.
doi:10.1364/OE.20.005882
[23] Husu, H., Siikanen, R., Mäkitalo, J., Lehtolahti, J., Laukkanen, J., Kuittinen, M., and Kauranen, M., "Metamaterials with Tailored Nonlinear Optical Response," *Nano Letters*, Vol. 12, No. 2, 2012, pp. 673–677.
doi:10.1021/nl203524k
[24] Montelongo, Y., Tenorio-Pearl, J. O., Milne, W. I., and Wilkinson, T. D., "Polarization Switchable Diffraction Based on Subwavelength Plasmonic Nanoantennas," *Nano Letters*, Vol. 14, No. 1, 2013, pp. 294–298.
doi:10.1021/nl4039967
[25] Syrenova, S., Wadell, C., and Langhammer, C., "Shrinking-Hole Colloidal Lithography: Self-Aligned Nanofabrication of Complex Plasmonic Nanoantennas," *Nano Letters*, Vol. 14, No. 5, 2014, pp. 2655–2663.
doi:10.1021/nl500514y
[26] Menzel, C., Helgert, C., Rockstuhl, C., Kley, E. B., Tünnermann, A., Pertsch, T., and Lederer, F., "Asymmetric Transmission of Linearly Polarized Light at Optical Metamaterials," *Physical Review Letters*, Vol. 104, No. 25, 2010, Paper 253902.
doi:10.1103/PhysRevLett.104.253902
[27] Pfeiffer, C., Zhang, C., Ray, V., Guo, L. J., and Grbic, A., "High Performance Bianisotropic Metasurfaces: Asymmetric Transmission of Light," *Physical Review Letters*, Vol. 113, No. 2, 2014, Paper 023902.
doi:10.1103/PhysRevLett.113.023902
[28] Grady, N. K., Heyes, J. E., Chowdhury, D. R., Zeng, Y., Reiten, M. T., Azad, A. K., Taylor, A. J., Dalvit, D. A. R., and Chen, H.-T., "Terahertz Metamaterials for Linear Polarization Conversion and Anomalous Refraction," *Science*, Vol. 340, No. 6138, 2013, pp. 1304–1307.
doi:10.1126/science.1235399
[29] Luk'yanchuk, B., Zheludev, N. I., Maier, S. A., Halas, N. J., Nordlander, P., Giessen, H., and Chong, C. T., "The Fano Resonance in Plasmonic Nanostructures and Metamaterials," *Nature Materials*, Vol. 9, No. 9, 2010, pp. 707–715.
doi:10.1038/nmat2810
[30] Howell, J. R., Siegel, R., and Menguc, M. P., *Thermal Radiation Heat Transfer*, 5th ed., Taylor and Francis, New York, 2010, pp. 60–61.
[31] Lee, B. J., Zhang, Z. M., Early, E. A., DeWitt, D. P., and Tsai, B. K., "Modeling Radiative Properties of Silicon with Coatings and Comparison with Reflectance Measurements," *Journal of Thermophysics and Heat Transfer*, Vol. 19, No. 4, 2005, pp. 558–565.
doi:10.2514/1.13596
[32] Cunnington, G. R., and Lee, S. C., "Radiative Properties of Fibrous Insulations—Theory Versus Experiment," *Journal of Thermophysics and Heat Transfer*, Vol. 10, No. 3, 1996, pp. 460–466.
doi:10.2514/3.811
[33] Baillis, D., Raynaud, M., and Sacadura, J. F., "Determination of Spectral Radiative Properties of Open Cell Foam: Model Validation," *Journal of Thermophysics and Heat Transfer*, Vol. 14, No. 2, 2000, pp. 137–143.
doi:10.2514/2.6519
[34] Husu, H., Mäkitalo, J., Laukkanen, J., Kuittinen, M., and Kauranen, M., "Particle Plasmon Resonances in L-Shaped Gold Nanoparticles," *Optics Express*, Vol. 18, No. 16, 2010, pp. 16,601–16,606.
doi:10.1364/OE.18.016601
[35] Capolino, F., *Applications of Metamaterials*, CRC Press, Boca Raton, FL, 2009, p. 8-2.
[36] Sakurai, A., Zhao, B., and Zhang, Z. M., "Effect of Polarization on Dual-Band Infrared Metamaterial Emitters or Absorbers," *Journal of Quantitative Spectroscopy and Radiative Transfer*, (in press) Dec. 2014.
doi:10.1016/j.jqsrt.2014.11.018
[37] Schubert, M., "Polarization-Dependent Optical Parameters of Arbitrarily Anisotropic Homogeneous Layered Systems," *Physical Review B: Solid State*, Vol. 53, No. 8, 1996, pp. 4265–4274.
doi:10.1103/PhysRevB.53.4265
[38] Yariv, A., and Yeh, P., *Optical Waves in Crystals: Propagation and Control of Laser Radiation*, Wiley-Interscience, New York, 2002, p. 121.
[39] Zhang, Z. M., *Nano/Microscale Heat Transfer*, McGraw–Hill, New York, 2007, p. 310.
[40] Moharam, M. G., Grann, E. B., Pommet, D. A., and Gaylord, T. K., "Formulation for Stable and Efficient Implementation of the Rigorous Coupled-Wave Analysis of Binary Gratings," *Journal of the Optical Society of America A*, Vol. 12, No. 5, 1995, pp. 1068–1076.
doi:10.1364/JOSAA.12.001068
[41] Born, M., and Wolf, E., *Principles of Optics*, 7th ed., Cambridge Univ. Press, Cambridge, England, U.K. 1999, p. 38.
[42] Azzam, R. M. A., and Bashara, N. M., *Ellipsometry and Polarized Light*, North Holland, Amsterdam, 1977, p. 272.
[43] Palik, E. D., *Handbook of Optical Constants of Solids*, Academic Press, San Diego, CA, 1985, p. 286.
[44] Wang, X. J., Haider, A. M., Abell, J. L., Zhao, Y.-P., and Zhang, Z. M., "Anisotropic Diffraction from Inclined Silver Nanorod Arrays on Grating Templates," *Nanoscale and Microscale Thermophysical Engineering*, Vol. 16, No. 1, 2012, pp. 18–36.
doi:10.1080/15567265.2011.646384